

Tailored utilization of acquired k -space points for GRAPPA reconstruction

Peng Qu, Gary X. Shen^{*}, Chunsheng Wang, Bing Wu, Jing Yuan

Department of Electrical and Electronic Engineering, The University of Hong Kong, Pokfulam, Hong Kong

Received 30 August 2004; revised 14 January 2005

Abstract

The generalized auto-calibrating partially parallel acquisition (GRAPPA) is an auto-calibrating parallel imaging technique which incorporates multiple blocks of data to derive the missing signals. In the original GRAPPA reconstruction algorithm only the data points in phase encoding direction are incorporated to reconstruct missing points in k -space. It has been recognized that this scheme can be extended so that data points in readout direction are also utilized and the points are selected based on a k -space locality criterion. In this study, an automatic subset selection strategy is proposed which can provide a tailored selection of source points for reconstruction. This novel approach extracts a subset of signal points corresponding to the most linearly independent base vectors in the coefficient matrix of fit, effectively preventing incorporating redundant signals which only bring noise into reconstruction with little contribution to the exactness of fit. Also, subset selection in this way has a regularization effect since the vectors corresponding to the smallest singular values are eliminated and consequently the condition of the reconstruction is improved. Phantom and in vivo MRI experiments demonstrate that this subset selection strategy can effectively improve SNR and reduce residual artifacts for GRAPPA reconstruction.

Published by Elsevier Inc.

Keywords: Parallel imaging; SMASH; GRAPPA; RF coil array; Image reconstruction

1. Introduction

Parallel imaging has been one of the most popular topics in MRI research in recent years for its potential to speed up MRI scanning. By using sensitivity information from a RF coil array to perform some of the spatial encoding which is traditionally accomplished by magnetic field gradient, parallel imaging techniques allow reduction of phase encoding steps and consequently decrease the scan time.

Following early proposals for parallel imaging in the late 1980s [1,2], several practical reconstruction strategies have been proposed, such as sensitivity encoding (SENSE) [3], simultaneous acquisition of spatial har-

monics (SMASH) [4,5], parallel imaging with localized sensitivities (PILS) [6], and sensitivity profiles from an array of coils for encoding and reconstruction in parallel (SPACE RIP) [7]. SMASH is the first experimentally successful parallel imaging technique which relies on the ability to approximate low-order harmonics of the desired field of view (FOV) by linear combinations of sensitivity functions. Several more flexible strategies have been proposed to improve the performance of SMASH in recent years, which include the tailored SMASH [8], AUTO-SMASH [9] and later VD-AUTO-SMASH [10], the coil-by-coil SMASH [11], the generalized SMASH [12], and the SENSE/SMASH hybrid approach proposed by Sodickson and McKenzie [13].

The generalized auto-calibrating partially parallel acquisition (GRAPPA) [14] is an improved SMASH-type technique which essentially combines several advantages

^{*} Corresponding author. Fax: +852 2559 8738.

E-mail address: gxshen@eee.hku.hk (G.X. Shen).

of the previous improvements to SMASH, including auto-calibration, coil-by-coil reconstruction, and incorporating multiple data blocks. In GRAPPA, a block-wise reconstruction procedure is implemented. For producing each missing line in k -space for each single channel, multiple lines from all channels are utilized. Since more information is incorporated to reconstruct missing lines, GRAPPA can substantially improve the accuracy of fit and extend the types of coil arrays and FOV orientations.

One limitation of the original GRAPPA is that the utilization of acquired k -space data to reconstruct each specific missing point is restricted within the phase encoding (PE) direction. In Sodickson's work previous to GRAPPA [13] it has been suggested that each acquired k -space point can be incorporated in reconstruction, including the data points in frequency encoding (FE) direction. A simple method to select a k -space subset in GRAPPA reconstruction is the so-called k -space locality criterion, as proposed by Yeh et al. [15], in which signal data are included in the generalized encoding matrix (GEM) based on their distances from the target point. However, how to select an optimal k -space subset in reconstruction is still an unsettled question. In this study, first we compare two reconstruction schemes in various situations by simulations, revealing that the optimal k -space subset in GRAPPA should depend on the coil array configuration and the orientation of FOV; second we propose an automatic subset selection routine based on matrix decompositions. In contrast to the simple locality criterion, this new approach extracts a tailored subset of signal points corresponding to the most linearly independent base vectors in the coefficient matrix of fit, effectively preventing incorporating redundant signals which only bring noise into reconstruction without contribution to the exactness of fit. Also, subset selection in this way has a regularization effect since the columns corresponding to the smallest singular values are eliminated and consequently the condition of the reconstruction is improved.

2. Materials and methods

2.1. General view of k -space reconstruction in parallel MRI

The MR signal from a two-dimensional slice detected by a given RF coil can be written as

$$S_\rho(K_x, K_y) = \iint_{x,y} dx dy C_\rho(x, y) M(x, y) \times \exp\{-i(k_x x + k_y y)\}, \quad (1)$$

where $M(x, y)$ represents the spin density in a two-dimensional image plane labeled by Cartesian coordinates x and y , $C_\rho(x, y)$ represents the RF sensitivity for the ρ th

component coil in the array, and k_x, k_y are k -space coordinates. The encoding functions for MR signals consist of coil sensitivity modulation and gradient modulation in two directions [13]

$$B_\rho(x, y, k_x, k_y) = C_\rho(x, y) \exp(-ik_x x) \exp(-ik_y y). \quad (2)$$

Substituting Eq. (2) into Eq. (1) and written in matrix notation

$$S = BM. \quad (3)$$

Multiple coil reconstruction is essentially a problem of how to invert the encoding matrix B . From this perspective, Sodickson and McKenzie [13] have provided a general view to parallel MRI and disclosed the relationship between SENSE and SMASH. In SMASH-type techniques, missing harmonics associated with omitted k -space positions are filled in by an 'inverse/fit' process before the final FFT. Specifically, in SMASH, harmonics of different orders are generated by weighted combinations of coil sensitivity profiles

$$\sum_{\rho=1}^L n_\rho^{(m)} C_\rho(x, y) \approx \exp(-im\Delta k_y y) \quad (4)$$

with L representing the number of coil elements, and m the order of the harmonics. Then the combinations of component coil signals with the same weights can be used to approximate the shifted signals

$$\sum_{\rho=1}^L n_\rho^{(m)} S_\rho(k_x, k_y) \approx S(k_x, k_y + m\Delta k_y). \quad (5)$$

If the fitting scheme in SMASH is expanded so that more than one acquired data points are used to reconstruct each missing point, Eq. (4) can be extended to

$$\sum_{\rho=1}^L \sum_{(\lambda_x, \lambda_y)} n_{\rho, (\lambda_x, \lambda_y)}^{(m)} C_\rho(x, y) \exp(-i\lambda_x \Delta k_x x) \exp(-i\lambda_y \Delta k_y y) \approx \exp(-im\Delta k_y y). \quad (6)$$

Here λ_x and λ_y are numbers related to the relative shifts from the acquired points to the target point. Correspondingly, Eq. (5) can be extended to

$$\sum_{\rho=1}^L \sum_{(\lambda_x, \lambda_y)} n_{\rho, (\lambda_x, \lambda_y)}^{(m)} S_\rho(k_x - \lambda_x \Delta k_x, k_y - \lambda_y \Delta k_y) \approx S(k_x, k_y + m\Delta k_y). \quad (7)$$

Eq. (7) implies that each acquired k -space point can be utilized to derive each missing point.

2.2. Comparison of two reconstruction schemes

The flexibility in selecting acquired k -space points in GRAPPA reconstruction raises the question of how to choose an optimal subset. A natural and usually employed criterion is the locality criterion which assumes

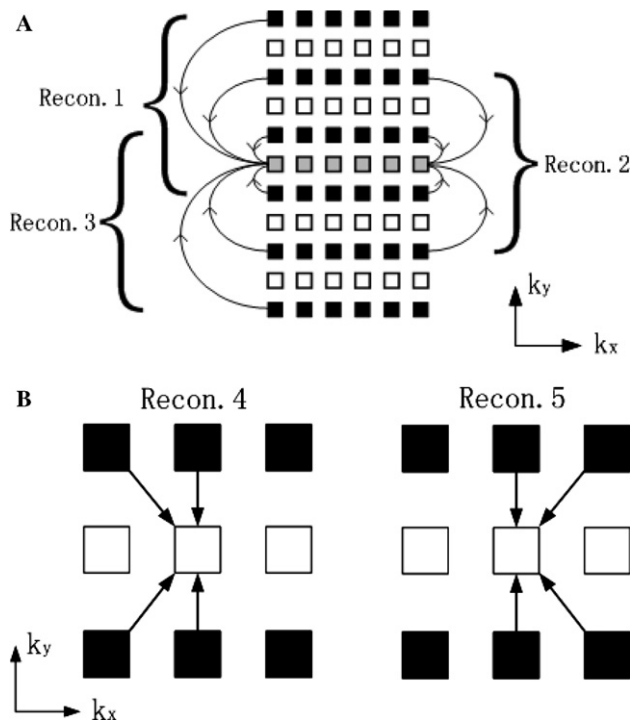


Fig. 1. Graphic illustration of the original GRAPPA and the extended GRAPPA. (A) The original GRAPPA, only points in PE direction are incorporated. The three reconstructions are combined each incorporates four data blocks. (B) The extended GRAPPA, the k -space locality criterion is applied. The two reconstructions are combined each incorporates four neighbor points.

that the nearest points have the largest contribution in deriving the missing point. However, this assumption is not proven exactly correct. In this study, we remark that the source points in PE direction and FE direction usually have different contributions in the fit and their contributions highly depend on the coil array configuration and FOV orientation. To demonstrate this, two reconstruction schemes, as sketched in Fig. 1, are compared in various situations. The first is an original GRAPPA reconstruction which only uses points in PE direction, and the second is an extended GRAPPA reconstruction which makes use of several neighbor signal points based on the k -space locality criterion. Specifically, in the original GRAPPA, the three reconstruction schemes sketched in Fig. 1A were implemented (labeled as Recon1, Recon2, and Recon3, respectively); in the extended GRAPPA, the two reconstruction schemes sketched in Fig. 1B (labeled as Recon4, Recon5, respectively) were implemented. In both cases their different reconstruction results were combined weighted by the goodness of fits. Computer simulations of phantom imaging were performed to compare both reconstruction strategies.

2.3. An automatic routine for subset selection

As described above, the optimal k -space subset for GRAPPA is not necessarily the nearest points, and its

selection should depend on different situations, e.g., FOV, coil configurations. Therefore, it is highly necessary to have an adaptive routine to automatically identify the most efficient subset to include in the reconstruction. For this purpose we propose a novel two-stage method for subset selection. In the first stage a relatively larger range of local data blocks are incorporated to form the coefficient matrix of fit, then in the second stage a subset corresponding to the most linearly independent columns is extracted from them based on the numerical characteristic of the matrix.

The key procedure in GRAPPA is an ‘inverse/fit’ process which can be formulated as a least squares problem. Here we denote it in a simple matrix notation

$$Ax = b, \quad (8)$$

where A and b are formed by alignment of ACS points and x is the vector of reconstruction parameters. A has $N_c \times N_s$ columns with N_c denoting the number of coils and N_s denoting the number of source points to include in reconstructing a missing point. The basic idea of our approach is first incorporating a larger range of local source points to form the matrix A and then extract a number of most linearly independent columns from A for calibration and reconstruction. Here we denote the number of initially included k -space points (positions) by N_{initial} and denote the number of columns extracted by N_{select} . Note that N_{select} can be freely chosen and is not necessarily a multiple of N_c or N_s . If all columns of A are retained, $N_{\text{select}} = N_{\text{initial}} \times N_c$. In practice N_{select} should be determined by the compromise between accuracy of fit and computation time. This strategy has two benefits. First, it can select a most efficient subspace of A for the fit and leave out the most likely redundant signals. Second, the columns eliminated by this strategy correspond to the smallest singular values of A . As such, the condition of A can be improved and reconstructions can become more stable in presence of noise. Selection of the most linearly independent columns can be achieved by linear algebra tools such as singular value decomposition (SVD) and rank-revealing QR decomposition (RRQR) [16]. Since the SVD method always involves much larger computational effort, in our implementations the RRQR method was employed in favor of computational efficiency. Detailed description of the RRQR algorithm is presented in Appendix A. In this study the effectiveness of this approach is demonstrated by both phantom and in vivo experiments and its performance is compared with the simple k -space locality criterion.

2.4. Computer simulation

Computer simulations were performed to compare the two reconstruction schemes sketched in Fig. 1 for two different coil configurations. One is a 4-element spine coil array aligned in head-foot direction which is

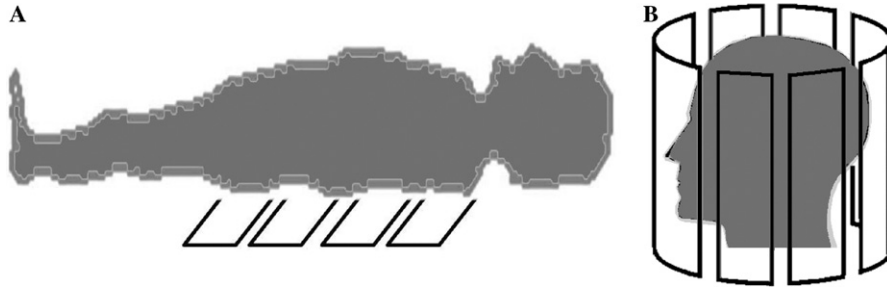


Fig. 2. Sketch of the two coil arrays used for comparing the performance of the original GRAPPA and the extended GRAPPA. (A) The 4-element spine array for coronal imaging; (B) The 8-element head array for axial imaging.

sketched in Fig. 2A. In this study, it is used for a coronal FOV. The other is a circularly arranged 8-element head coil for brain imaging which is sketched in Fig. 2B, and it is used for an axial FOV. Sensitivity profiles of these coils with the given FOVs are simulated using an analytic integration of Biot-Savart equation. Then these coil sensitivities were used with a standard Shepp–Logan phantom image produced by MATLAB to generate full versions of k -space datasets (matrix = 128×128). Simulated raw data with different acceleration factors were then created by extracting partial datasets from the full datasets. To compare the two reconstruction schemes sketched in Fig. 1, first their goodness of fits was evaluated for both arrays with varying acceleration factors. The accuracy of fit was estimated by the maximum and mean values of the fitting errors for a particular auto-calibrating signals (ACS) line. Then both the original GRAPPA and the extended GRAPPA were performed with the simulated k -space data and their reconstruction results are presented for comparison. Algorithms were all implemented in the MATLAB programming environment on a Pentium M 2.0G computer with 512M ram.

2.5. MRI experiments

MRI experiments were performed on a 3T Siemens Trio MRI system equipped with eight independent receiver channels. All raw data were acquired with body coil as transmit coil and an 8-leg band-pass birdcage head coil as receive coil which is tuned to resonate as eight independent loops to form an 8-element coil array. So this head coil is similar with the simulated array in Fig. 2B except that it is closed on the top (i.e., the elements curve in together at the top of the head).

Transverse phantom images were acquired with a turbo spin echo sequence (FOV = 200×200 mm, matrix = 256×256 , slice thickness = 5 mm, TE = 6.8 ms, TR = 0.7 s). In this experiment, a full dataset was acquired and later decimated off-line by a factor of 1.8 (outer reduction factor (ORF) = 2 [10], 10 ACS lines) and 2.7 (ORF = 3, 10 ACS lines) to simulate 1.8- and 2.7-fold acceleration, respectively.

Sagittal brain images were acquired using an inversion recovery FLASH sequence (FOV = 256×256 mm, matrix = 256×256 , TE = 2.7 ms, TR = 2.1 s, TI = 1.1 s, flip angle = 12°) with 2.7-fold acceleration (ORF = 3, 10 ACS lines in the central k -space were acquired for auto-calibration).

The automatic subset selection routine was employed in GRAPPA reconstruction for both phantom and in vivo experiments. At first 8×8 blocks of local data were incorporated to form the matrix A in Eq. (8) with $8 \times 8 \times 8$ columns. Then we extracted the 16×8 most linearly independent columns of A by RRQR algorithm and used this sub-matrix to replace the original matrix A for the fit. To demonstrate the effectiveness of this approach, we also performed an ordinary GRAPPA reconstruction as a reference which used 4×4 blocks (thus A also had 16×8 columns) based on the locality criterion.

3. Results

The results of computer simulations are summarized in Table 1 and Fig. 3.

3.1. Comparison of fitting accuracy

The results of auto-calibration of the five reconstruction schemes in Fig. 1 with the two coil arrays in Fig. 2 for different acceleration factors are listed in Table 1. All the numbers have been scaled by a same factor since their relative values are more meaningful. The fitting error is defined by the difference between target ACS data and least-squares fit results. Table 1 shows that the reconstructions involved in the extended GRAPPA have larger fitting errors than those involved in original GRAPPA for the 4-element planar spine array; while for the 8-element head coil array, the calibrations of the extended GRAPPA are more accurate. Since the goodness of fit is related to the residual aliasing artifact, it is expected that the extended GRAPPA works better than original GRAPPA for the circularly arranged head array, while for the planar array where coil sensitivity

Table 1
Comparison of fitting accuracy by simulations: Original GRAPPA vs. extended GRAPPA

Acceleration	2×					3×				
	O-GRAPPA			E-GRAPPA		O-GRAPPA			E-GRAPPA	
	Recon1	Recon2	Recon3	Recon4	Recon5	Recon1	Recon2	Recon3	Recon4	Recon5
<i>S-array</i>										
Error-max	108	107	92	156	113	358	350	328	271	144
Error-mean	12	12	6.1	22	15	18	22	8.9	30	16
<i>H-array</i>										
Error-max	21	14	17	2.3	2.6	184	115	140	11	12
Error-mean	3.6	2.3	3.0	0.37	0.57	33	28	31	0.98	1.5

Different reconstructions (Recon1–5) are sketched in Fig. 2.

S-array: the 4-element spine coil; H-array: the 8-element head coil; O-GRAPPA: original GRAPPA; E-GRAPPA: extended GRAPPA.

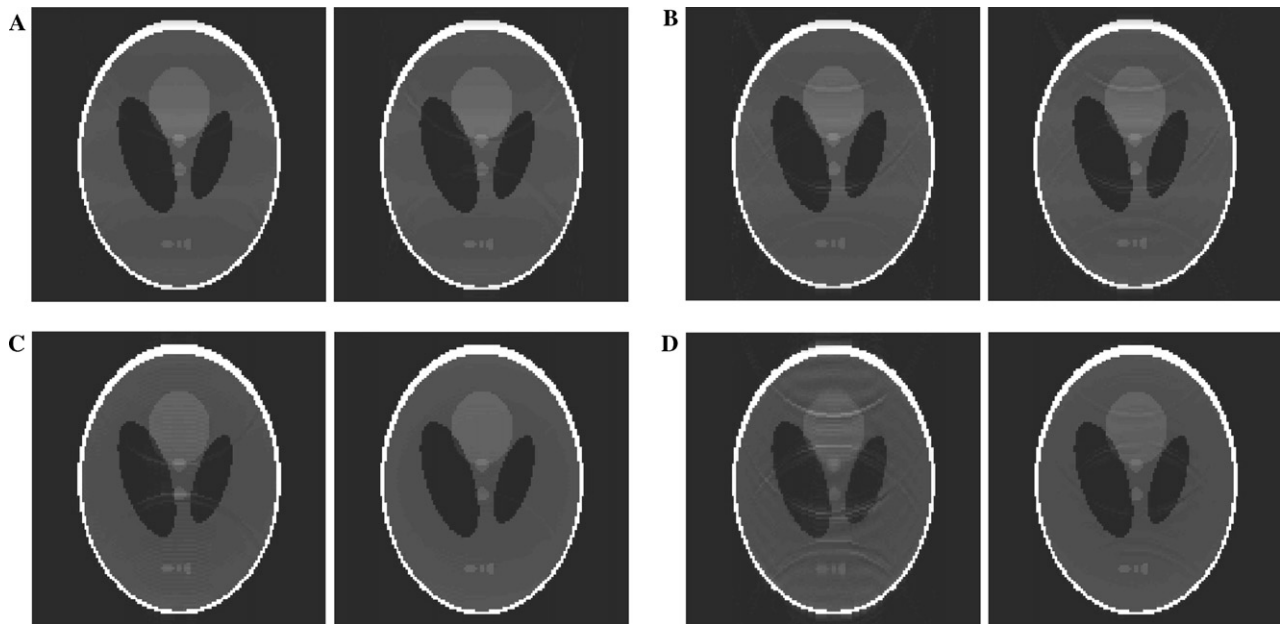


Fig. 3. Simulated reconstruction results of a Shepp–Logan phantom image with the original GRAPPA (left) and the extended GRAPPA (right). (A) $R = 1.7$, with the 4-element spine array; (B) $R = 2.4$, with the 4-element spine array; (C) $R = 1.7$, with the 8-element head array; and (D) $R = 2.4$, with the 8-element head array. In each reconstruction 10 ACS lines are used for calibration.

profiles are aligned only in phase encoding direction, the original GRAPPA reconstruction is more suitable.

3.2. Comparison of reconstruction results

The simulated reconstruction results of the two reconstruction strategies in Fig. 1 are presented in Fig. 3. The images with the 4-element spine coil are shown in Fig. 3A ($R = 1.7$, ORF = 2, 10 ACS lines) and Fig. 3B ($R = 2.4$, ORF = 3, 10 ACS lines), and the images with the 8-element head coil are shown in Fig. 3C ($R = 1.7$) and Fig. 3D ($R = 2.4$). As expected, for the spine array, the original GRAPPA reconstruction yields slightly better image quality than extended GRAPPA; while for the head array, the extended GRAPPA performs better than the original GRAPPA. Particularly, with net acceleration factor $R = 2.4$, the image produced by the original GRAPPA suffers from noticeable alias-

ing artifacts, while in the extended GRAPPA these artifacts are significantly reduced.

3.3. MRI experiments

Reconstruction results from the phantom imaging are displayed in Fig. 4. Here Figs. 4A and B are the reconstructed images using the ordinary GRAPPA incorporating local 4×4 data blocks with $R = 1.8$ (ORF = 2, 10 ACS lines) and $R = 2.7$ (ORF = 3, 10 ACS lines), respectively. Figs. 4C and D are their counterparts using the automatic subset selection routine. Low level of residual aliasing artifacts exist in all these images, but it is clear that GRAPPA with the automatic subset selection strategy is more effective to suppress these artifacts.

Images from In vivo experiments are shown in Fig. 5. The ordinary GRAPPA reconstruction result using k -space locality criterion is shown in Fig. 5A, and the

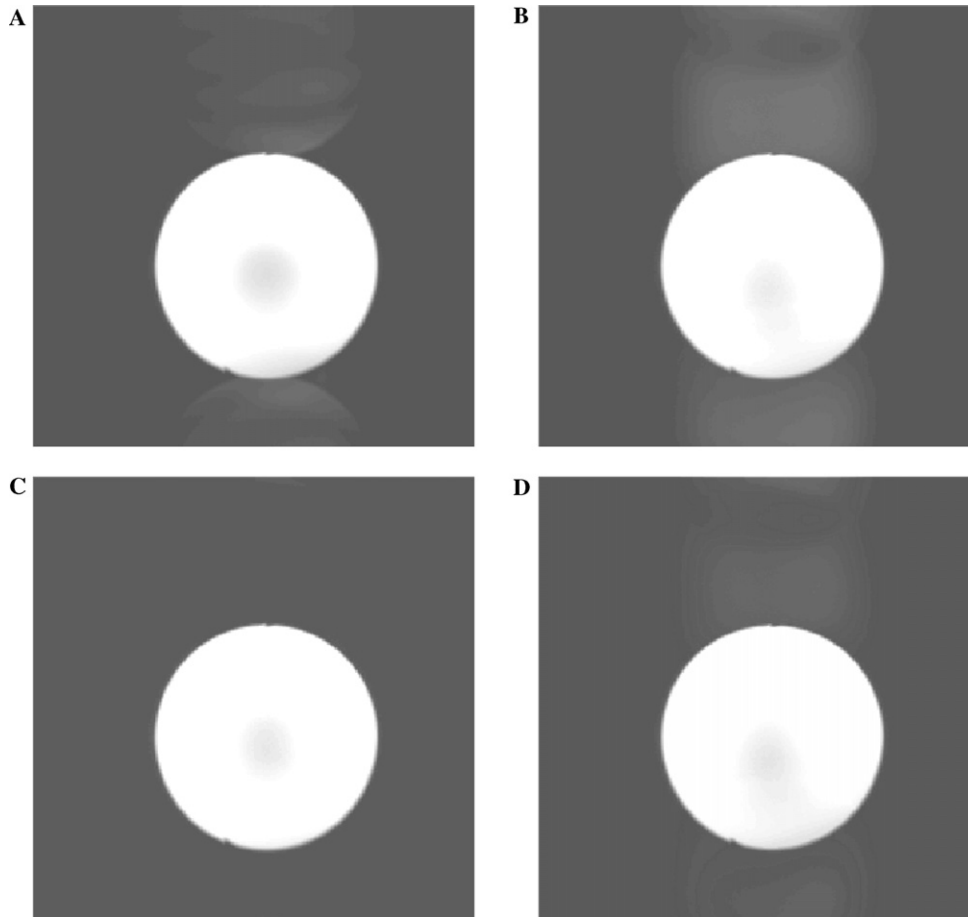


Fig. 4. GRAPPA reconstruction results of a phantom image using different selection of k -space subset. (A) Ordinary GRAPPA image incorporating local 4×4 data blocks with $R = 1.8$; (B) ordinary GRAPPA image incorporating local 4×4 data blocks with $R = 2.7$; (C) GRAPPA image using automatic subset selection approach with $R = 1.8$; and (D) GRAPPA image using automatic subset selection approach with $R = 2.7$. Ten ACS lines are used for calibration in all reconstructions. For (C and D) $N_{\text{initial}} = 8 \times 8$, $N_{\text{select}} = 16 \times 8$.

result using automatic subset selection is shown in Fig. 5B. To provide a visual impression of the SNR of both reconstructions, small regions (50×50 pixels) of the two images (as indicated by the white box in Figs. 5A and B) are extracted and highlighted in Figs. 5C and D. It is demonstrated that the automatic subset selection method can yield better SNR for GRAPPA reconstructions than the simple k -space locality criterion.

4. Discussion

This study has shown that the ordinary k -space locality criterion is not an optimal means for utilization of data points in GRAPPA in some cases. An automatic subset selection strategy based on matrix decomposition has been proposed. Two important parameters have to be carefully considered in implementation of this method. The first parameter is N_{select} , i.e., how many points, or, how many independent columns of matrix A should be selected in the reconstruction. The second parameter is N_{initial} , i.e., how large the initial range of data blocks

should be. These two parameters should be determined considering both the accuracy of reconstruction and computational efficiency. Generally increasing N_{select} can improve the exactness of fit and consequently reduce residual artifacts. However, in our experience when more than 16 data blocks are used, no obvious improvement of fit was observed with increasing number of data blocks. This is especially the case if the number of coils is large. The computation time of the GRAPPA algorithm, on the other hand, increases significantly with the increase of N_{select} . To provide a reference, we conducted GRAPPA algorithm with different N_{select} and the time costs of the reconstructions are listed in Table 2. From the regularization point of view, N_{select} essentially plays the role of regularization parameter. In this sense, some parameter choice approaches, such as L-curve and the generalized cross-validation (GCV) [16] can be potentially useful for automatic selection and optimization of N_{select} for a given reconstruction quality. Quantitative study of this issue is currently under way. Obviously the initial range N_{initial} should cover a sufficient range to guarantee that the most useful points

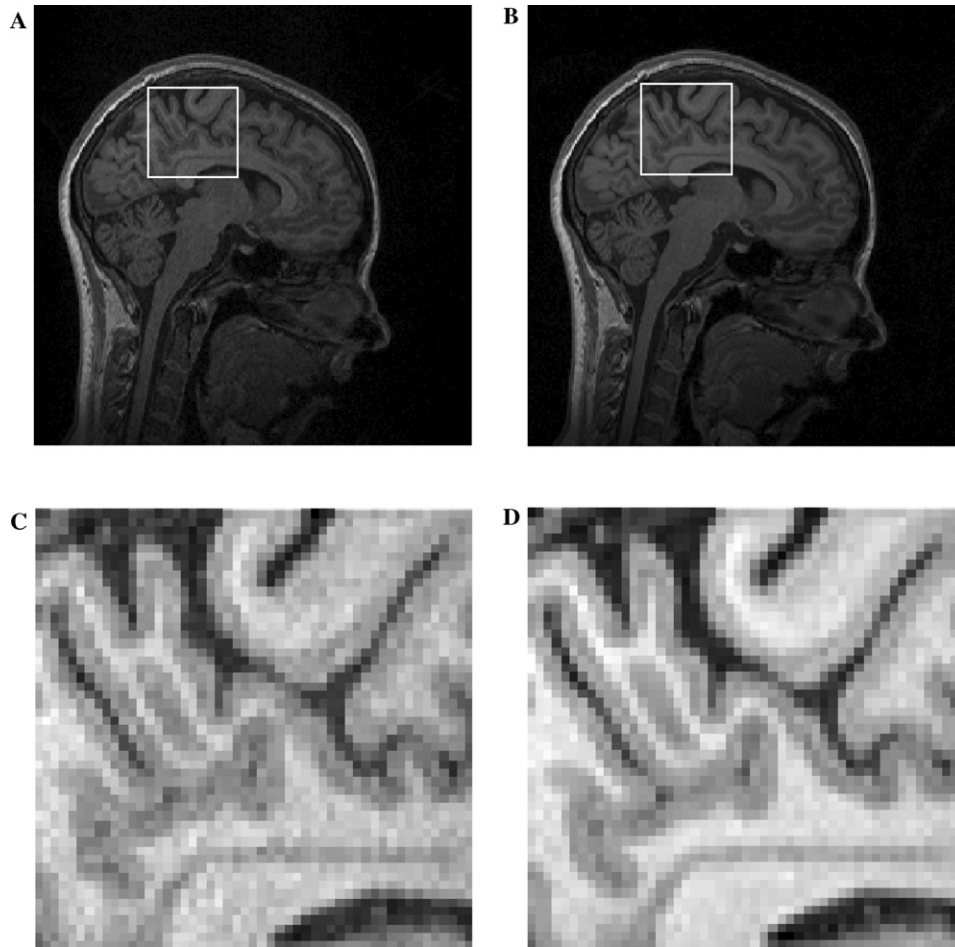


Fig. 5. $3\times$ GRAPPA reconstruction results of sagittal brain images (10 ACS lines, net acceleration factor = 2.7). (A) Ordinary GRAPPA image incorporating local 4×4 data blocks; (B) GRAPPA image using automatic subset selection approach, $N_{\text{initial}} = 8\times 8$, $N_{\text{select}} = 16\times 8$; (C and D) highlighted 50×50 regions extracted from (A and B) (indicated by the white boxes) respectively.

Table 2

Computation time vs. number of k -space points incorporated for GRAPPA reconstruction

No. of points incorporated	Time cost for deriving the reconstruction parameters (s)	Total time cost for reconstruction (s)
2×2	0.11	8.7
3×3	0.25	9.9
4×4	0.98	11.9
5×5	2.18	14.4
6×6	5.40	19.6

Matrix = 256×256 , $R = 2$, 10 ACS lines for calibration, algorithms implemented on a Pentium-M 2.0G computer with 512M ram.

for reconstruction are included. N_{initial} should be related to N_{select} and empirically a N_{initial} equal to four times of N_{select}/N_c is sufficient to cover the “potentially useful” points. N_{initial} also affects the computation time since the algorithm involves an RRQR decomposition of matrix A (see Eq. (8)), but it is not dominant. In our experiments, the implementation of the RRQR algorithm to extract 16×8 columns from $8\times 8\times 8$ columns of A took around 1.6 s.

The nature of all the SMASH-like techniques is the data shift in k -space. A specific set of relative shifts from the acquired data points to the specific target point corresponds to a set of weights for combination of those acquired data points to yield that target point [17]. As introduced in some previous work [12,18–20], k -space based reconstruction methods are not limited to Cartesian trajectories. Adapted implementations of GRAPPA for radial and spiral trajectories have been reported recently by Griswold et al. [18] and Heberlein et al. [19], respectively. In both of their methods the acquired data are aligned along the trajectories and segmented, and for each segment the conventional GRAPPA is performed. The subset selection approach proposed in this study could also be effective for non-Cartesian GRAPPA.

5. Conclusion

Computer simulations have demonstrated that the optimal selection of data points in GRAPPA reconstruc-

tion should depend on the coil configuration and FOV orientation. An automatic subset selection approach has been proposed to improve the performance of GRAPPA reconstruction. This novel method can effectively prevent incorporating redundant signals and also has a regularization effect for better numerical conditioning of the inverse problem. Phantom and in vivo experiments have demonstrated that the automatic routine for selecting a tailored subset has significant potential for suppressing aliasing artifacts and improving SNR.

Acknowledgments

The authors thank Mr. Mike Rohan, Harvard Medical School, for his help with the in vivo experiments. This work was supported by Hong Kong RGC Earmarked Research Grant HKU 7045/01E and HKU 7170/03E.

Appendix A. Rank-revealing QR decomposition

The rank-revealing QR (RRQR) decomposition is a special QR factorization with column pivoting which is guaranteed to reveal the numerical rank of a matrix [16]. Let A is an $m \times n$ matrix ($m > n$), our object is to extract r most linearly independent columns in A . Generally its RRQR decomposition has the following form:

$$A\Pi = QR = (Q_1, Q_2) \begin{pmatrix} R_{11} & R_{12} \\ 0 & R_{22} \end{pmatrix},$$

where Π is a permutation matrix, Q has orthonormal columns, R_{11} is an $r \times r$ triangular matrix and R_{22} is a $(n-r) \times (n-r)$ triangular matrix. The goal of RRQR decomposition is to maximize the smallest singular value of R_{11} . This goal is achieved by the permutation matrix Π , namely, the ordinary column pivoting strategy.

An explicit RRQR algorithm is described as follows [21]:

- (1) Input $A = [a_{ij}] \in R^{m \times n}$; $p_j = j$, $\gamma_j = \|a_j\|$, $j = 1, 2, \dots, n$, $k = 1$.
- (2) Determine l , so that $\gamma_l = \max_{k \leq j \leq n} \gamma_j$.
- (3) If $k = r$, break and end the algorithm; otherwise go to the next step.
- (4) Interchange γ_l and γ_k , a_{il} and a_{ik} , $i = 1, 2, \dots, m$.
- (5) Determine a Householder transformer H_k , so that

$$H_k \begin{bmatrix} a_{kk} \\ \vdots \\ a_{mk} \end{bmatrix} = \begin{bmatrix} * \\ 0 \\ \vdots \\ 0 \end{bmatrix}.$$

- (6) $A = \text{diag}(I_{k-1}, H_k)A$, $\gamma_j = \gamma_j a_{kj}^2$, $j = k+1, \dots, n$.
- (7) $k = k+1$, go to step (2).

References

- [1] J.W. Carlson, An algorithm for NMR imaging reconstruction based on multiple RF receiver coils, *J. Magn. Reson.* 74 (1987) 376–380.
- [2] M. Hutchinson, U. Raff, Fast MRI data acquisition using multiple detectors, *Magn. Reson. Med.* 6 (1998) 87–91.
- [3] K.P. Pruessmann, M. Weiger, M.B. Scheidegger, P. Boesiger, SENSE: Sensitivity encoding for fast MRI, *Magn. Reson. Med.* 42 (1999) 952–962.
- [4] D.K. Sodickson, W.J. Manning, Simultaneous acquisition of spatial harmonics (SMASH): Fast imaging with radiofrequency coil arrays, *Magn. Reson. Med.* 38 (1997) 591–603.
- [5] R.F. Lee, C.R. Westgate, R.G. Weiss, P.A. Bottomley, An analytical SMASH procedure (ASP) for sensitivity-encoded MRI, *Magn. Reson. Med.* 43 (2000) 716–725.
- [6] M.A. Griswold, P.M. Jakob, R.M. Heidemann, A. Haase, Parallel imaging with localized sensitivities (PILS), *Magn. Reson. Med.* 44 (2000) 602–609.
- [7] W.E. Kyriakos, L.P. Panych, D.F. Kacher, C.F. Westin, C.M. Bao, R.V. Mulkern, F.A. Jolesz, Sensitivity profiles from an array of coils for encoding and reconstruction in parallel (SPACE RIP), *Magn. Reson. Med.* 44 (2000) 301–308.
- [8] D.K. Sodickson, Tailored SMASH image reconstructions for robust in vivo parallel MR imaging, *Magn. Reson. Med.* 44 (2000) 243–251.
- [9] P.M. Jakob, M.A. Griswold, R.R. Edelman, D.K. Sodickson, AUTO-SMASH: A self-calibrating technique for SMASH imaging, *MAGMA* 7 (1998) 42–54.
- [10] R.M. Heidemann, M.A. Ohliger, E.N. Yeh, M.D. Price, D.K. Sodickson, Coil-by-coil image reconstruction with SMASH, *Magn. Reson. Med.* 46 (2001) 619–623.
- [11] C.A. McKenzie, M.A. Ohliger, E.N. Yeh, M.D. Price, D.K. Sodickson, Coil-by-coil image reconstruction with SMASH, *Magn. Reson. Med.* 46 (2001) 619–623.
- [12] M. Bydder, D.J. Larkman, J.V. Hajnal, Generalized SMASH imaging, *Magn. Reson. Med.* 47 (2002) 160–170.
- [13] D.K. Sodickson, C.A. McKenzie, A generalized approach to parallel magnetic resonance imaging, *Med. Phys.* 28 (2001) 1629–1643.
- [14] M.A. Griswold, P.M. Jakob, R.M. Heidemann, M. Nittka, V. Jellus, J. Wang, B. Kiefer, A. Haase, Generalized auto-calibrating partially parallel acquisition (GRAPPA), *Magn. Reson. Med.* 47 (2002) 1202–1210.
- [15] E.N. Yeh, C.A. McKenzie, D. Lim, M.A. Ohliger, A.K. Grant, J.D. Willig, N. Rofsky, D.K. Sodickson, Parallel imaging with augmented radius in k -space (PARS), in: Proceedings of the ISMRM 10th Annual Meeting, #2399, 2002.
- [16] P.C. Hansen, Rank-deficient and discrete ill-posed problems: Numerical aspects of linear inversion, Philadelphia, SIAM, 1998.
- [17] M.A. Griswold, R.M. Heidemann, P.M. Jakob, The GRAPPA operator, in: Proceedings of the ISMRM 11th Annual Meeting, Toronto, 2003, pp. 459.
- [18] M.A. Griswold, R.M. Heidemann, P.M. Jakob, Direct parallel imaging reconstruction of radially sampled data using GRAPPA with relative shifts, in: Proceedings of the ISMRM 11th Annual Meeting, Toronto, 2003, pp. 459.
- [19] K.A. Heberlein, Y. Kadah, X. Hu, Segmented spiral parallel imaging using GRAPPA, in: Proceedings of the ISMRM 12th Annual Meeting, Tokyo, 2004, p. 75.
- [20] E.N. Yeh, M. Stuber, C.A. McKenzie, M.A. Ohliger, A.K. Grant, J.D. Willig, D.K. Sodickson, Self-calibrated spiral parallel imaging, in: Proceedings of the ISMRM 10th Annual Meeting, #2390, 2002.
- [21] A. Jennings, J.J. McKeown, Matrix Computation, Wiley, Chichester, England, 1991.